DOI: 10.17516/1997-1397-2022-15-6-730-741
УДК 535.39:535.34

Surface Plasmon-Polaritons In A Two-Layer Graphene Structure With A Dielectric Barrier Layer Under Various Control Regimes

Dmitry A. Evseev*
Svetlana V. Eliseeva†
Anatolij M. Shutyi‡
Dmitry I. Sementsov§
Ulyanovsk State University
Ulyanovsk, Russian Federation

Received 02.9.2022, received in revised form 05.10.2022, accepted 20.11.2022

Abstract. The dispersion dependences of a symmetric dielectric waveguide with graphene plates were compared in two regimes of graphene potential control from two sides of the structure. A general dispersion relation was obtained, the numerical analysis of which reveals the possibility of controlling the parameters of amplified surface modes. A numerical analysis of the dispersion relation solutions in the case of symmetry and asymmetry of the control potential on graphene layers has been carried out. A solution has been found that grows in amplitude with time in the region of negative conductivity of graphene in the presence of an inverse population of the levels.

Keywords: doped and inverted graphene, terahertz frequency range, symmetrical planar structure, chemical potential, real and imaginary parts of the propagation constant, amplification.

Citation: D.A. Evseev, S.V. Eliseeva, A.M. Shutyi, D.I. Sementsov, Surface Plasmon-Polaritons In A Two-Layer Graphene Structure With A Dielectric Barrier Layer Under Various Control Regimes, J. Sib. Fed. Univ. Math. Phys., 2022, 15(6), 730–741. DOI: 10.17516/1997-1397-2022-15-6-730-741.

Introduction

The formation of plasma waves in a graphene structure makes it possible to localize an electromagnetic field near graphene layers and significantly increase the efficiency of its interaction with the structure [1–12]. When charge carrier inversion is realized as a result of optical or injection pumping in graphene in the THz range, negative conductivity arises, the presence of which can lead to stimulated generation of THz plasmons and the possibility of amplifying radiation by inverted graphene [13–18].

Waveguide structures whose dispersion properties can be controlled by an external field are of considerable interest for applied photonics. One possible solution to this is to use layers of graphene as control electrodes. In a structure consisting of two parallel layers of graphene separated by a thin dielectric barrier layer, the electromagnetic fields of plasmons propagating

*comrade-dmitriy@mail.ru
† https://orcid.org/0000-0002-8288-4158
‡shuty@mail.ru
§ https://orcid.org/0000-0001-6760-0156

in these layers interact with each other, which leads to the formation of a single plasmon mode [19–24]. The parameters of structures containing graphene can be controlled by changing its chemical potential (Fermi energy) by an external electric field and creating an inverted state due to optical or injection pumping. In this work, we study the effect of the energy state of the graphene layers on the dispersion properties of a planar waveguide structure consisting of two graphene layers separated by a dielectric barrier layer. The dispersion characteristics for structures with layers of doped and inverted graphene are compared with a change in their energy state.

1. Structure and material parameters

Consider a planar dielectric waveguide with graphene plates. The dielectric permittivity of the barrier layer is ε_2, its thickness is d, for the coating medium and the substrate, the dielectric constants ε_1, ε_3 do not have dispersion and do not introduce losses. The surface conductivity of graphene, which depends on the chemical potential μ, is given by the Kubo formula [17, 25–27]:

$$\begin{aligned}\frac{\sigma_{dop}}{\sigma_0} &= \frac{8k_BT\tau}{\pi\hbar(1-i\omega\tau)}\ln\left[2\cosh\left(\frac{E_F}{2k_BT}\right)\right] + G\left(\frac{\hbar\omega}{2}, E_F\right) - R(\omega),\\ \frac{\sigma_{inv}}{\sigma_0} &= \frac{8k_BT\tau}{\pi\hbar(1-i\omega\tau)}\ln\left[1+\exp\left(\frac{E_F}{k_BT}\right)\right] + \tanh\left(\frac{\hbar\omega-2E_F}{4k_BT}\right) - R(\omega),\end{aligned} \tag{1}$$

$$G(\alpha,\beta) = \frac{\sinh(\alpha/k_BT)}{\cosh(\alpha/k_BT)+\cosh(\beta/k_BT)}, \quad R(\omega) = \frac{4\hbar\omega}{i\pi}\int_0^\infty \frac{G(E,E_F)-G(\hbar\omega/2,E_F)}{(\hbar\omega)^2-4E^2}dE.$$

where $\sigma_0 = e^2/4\hbar$, e is the charge of an electron, $\hbar$ and k_B are the Planck and Boltzmann constants, τ is the carrier scattering time, T is the temperature. Passive or unexcited graphene will be called, the chemical potential μ of which is zero, the valence band is completely filled, and the conduction band is free, there is no gap between the valence band and the conduction band. Active graphene has a non-zero chemical potential and can be in both equilibrium (doped) and non-equilibrium (inverted) states. The chemical potential is controlled by applying an external voltage between the graphene sheet and the substrate, which makes it possible to change the concentration of charge carriers and the filling of the bands, thereby changing the conductivity value [28–30].

Fig. 1 shows the frequency dependence of the real and imaginary parts of the conductivity of inverted graphene and doped graphene (solid and dashed lines), obtained at $T = 300\ K$, $\tau = 1\ ps$ (hereinafter) and values of the chemical potential $\mu = 0.10,\ 0.15,\ 0.20\ eV$ (curves 1–3), the value of $\mu = 0$ corresponds to the dotted curve. It is important that the real part of the conductivity in the terahertz region for inverted graphene takes negative values, while for doped graphene it is positive in the entire spectral range. The imaginary part for both types of the state of graphene remains positive over the entire frequency range and has a monotonically decreasing nature of the hyperbolic type.

2. Fields in the structure and the dispersion relation

The solution of the Maxwell equations for the specified waveguide structure will be sought in the form of a surface TM wave, the magnetic and electric fields of which decrease with distance

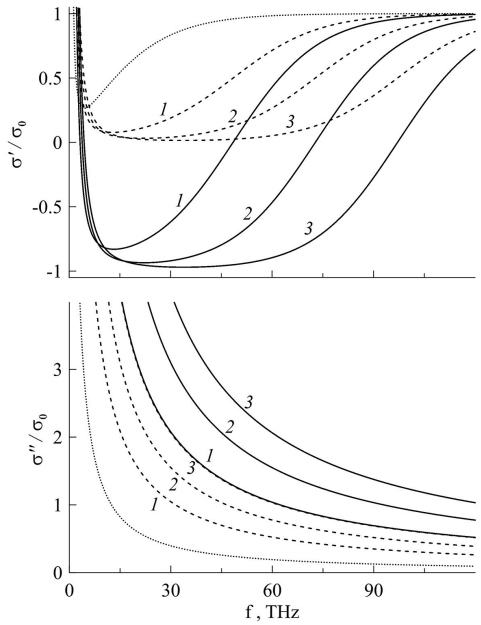

Fig. 1. Frequency dependence of the real and imaginary parts of the conductivity of inverted and doped graphene (solid and dashed lines), $\mu = 0,\ 0.10,\ 0.15,\ 0.20\ eV$ (dotted line, curves 1–3)

from the boundaries (graphene sheets):

$$H_y(t,x,z) = A_1 \exp\left(i(\omega\ t - \beta x)\right)\begin{cases} \exp\left(q_1 z\right), & z < 0, \\ A_2 \sinh\left(q_2 z\right) + A_3 \cosh\left(q_2 z\right), & 0 < z < d, \\ A_4 \exp\left(-q_3 z\right), & z > d, \end{cases} \tag{2}$$

$$E_x = -\frac{1}{ik_0\varepsilon_j}\frac{\partial H_y}{\partial z}, \quad E_z = \frac{1}{ik_0\varepsilon_j}\frac{\partial H_y}{\partial x}, \quad j = 1,\ 2,\ 3,$$

where $q_j = \sqrt{\beta^2 - k_0^2\varepsilon_j}$. Taking into account surface currents, the boundary conditions take the form:

$$\left[\vec{n}_{12}, (\vec{H}_1 - \vec{H}_2)\right] = \frac{4\pi\sigma_1}{c}\vec{E}_1, \quad \left[\vec{n}_{23}, (\vec{H}_2 - \vec{H}_3)\right] = \frac{4\pi\sigma_3}{c}\vec{E}_3,$$
$$\vec{n}_{12}(\vec{E}_1 - \vec{E}_2) = 0, \quad \vec{n}_{23}(\vec{E}_2 - \vec{E}_3) = 0. \tag{3}$$

From (2) and (3) we determine the constants A_{2-4}:

$$A_2 = \frac{\varepsilon_2 q_1}{\varepsilon_1 q_2}, \quad A_3 = 1 + i\frac{4\pi\sigma_1}{\omega}\frac{q_1}{\varepsilon_1}, \tag{4}$$

$$A_4 = -\frac{\varepsilon_3 q_2}{\varepsilon_2 q_3}\left(A_2 \cosh\left(q_2 d\right) + A_3 \sinh\left(q_2 d\right)\right)\exp\left(q_3 d\right),$$

the constant A_1 is normalizing for the field amplitude. Solving the boundary problem, we arrive at the following dispersion relation, which, taking into account the complexity of the parameters

included in it, determines the frequency dependence of the real and imaginary parts of the plasmon-polariton propagation constant for the structure under consideration:

$$\tanh(q_2 d) = -\frac{\left[\frac{\varepsilon_1 q_2}{\varepsilon_2 q_1}\left(1 + i\frac{4\pi\sigma_1}{\omega}\frac{q_1}{\varepsilon_1}\right)\right] + \left[\frac{\varepsilon_3 q_2}{\varepsilon_2 q_3}\left(1 + i\frac{4\pi\sigma_3}{\omega}\frac{q_3}{\varepsilon_3}\right)\right]}{1 + \left[\frac{\varepsilon_1 q_2}{\varepsilon_2 q_1}\left(1 + i\frac{4\pi\sigma_1}{\omega}\frac{q_1}{\varepsilon_1}\right)\right]\left[\frac{\varepsilon_3 q_2}{\varepsilon_2 q_3}\left(1 + i\frac{4\pi\sigma_3}{\omega}\frac{q_3}{\varepsilon_3}\right)\right]}. \tag{5}$$

Note that the general form of this dispersion relation does not depend on the energy state of the graphene layers, since it is determined by the parameters of the structure and the type of wave in it. In what follows, we confine ourselves to considering a structure for which $\varepsilon_1 = \varepsilon_3$ and, therefore, $q_1 = q_3$. In this case, the dispersion relation takes the form:

$$\tanh(q_2 d) = -\frac{2\frac{\varepsilon_1 q_2}{\varepsilon_2 q_1} + i\frac{4\pi q_2}{\omega\varepsilon_2}(\sigma_1 + \sigma_3)}{1 + \left(\frac{\varepsilon_1 q_2}{\varepsilon_2 q_1}\right)^2 - \left(\frac{4\pi q_2}{\omega\varepsilon_2}\right)^2 \sigma_1\sigma_3 + i\frac{4\pi q_2}{\omega\varepsilon_2}\frac{\varepsilon_1 q_2}{\varepsilon_2 q_1}(\sigma_1 + \sigma_3)}. \tag{6}$$

In expressions (5) and (6), the conductivity of each of the graphene layers depends on the chemical potential and quasi-Fermi energy (for doped graphene and inverted graphene, respectively), which can be controlled.

The completely symmetric situation ($\mu_1 = \mu_3$) allows us to additionally split equation (6) into two: for the antisymmetric and symmetric distribution of the longitudinal component of the electric field $E_x(z)$:

$$\coth\left(\frac{q_2 d}{2}\right) = -\frac{\varepsilon_1 q_2}{\varepsilon_2 q_1}\left(1 + i\frac{4\pi\sigma_1}{\omega}\frac{q_1}{\varepsilon_1}\right), \tag{7a}$$

$$\tanh\left(\frac{q_2 d}{2}\right) = -\frac{\varepsilon_1 q_2}{\varepsilon_2 q_1}\left(1 + i\frac{4\pi\sigma_1}{\omega}\frac{q_1}{\varepsilon_1}\right). \tag{7b}$$

The above equations coincide with those obtained in the paper [22].

3. Numerical simulation

The figures below show the results of numerical simulation of relations (6) and (7) for surface plasmon polaritons in structures with symmetric and asymmetric excitation of graphene layers. Here and below, the wave vector is normalized to the value $k_0 = k_B T/\hbar c \approx 1.3 \cdot 10^5\ cm^{-1}$, the barrier layer thickness $d = 10\ nm$. Fig. 2 shows the frequency dependence of the real and imaginary parts of the propagation constant in a symmetric structure with $\mu_1 = \mu_2 = \mu$, where the dashed curve corresponds to the unexcited state of graphene sheets, i.e. $\mu = 0$ curves 1–3 correspond to the values $\mu = 0.10,\ 0.15,\ 0.20\ eV$. Here, the solid curves correspond to the structure with inverted graphene, and the dashed curves correspond to doped graphene. It can be seen that with an increase in the chemical potential, the dispersion curves shift to the high-frequency region with an increase in the maximum values of the dependence $\beta'(\omega)$. For the structure with inverted graphene, there is a fairly wide frequency range, where $\beta''(\omega) < 0$ and reaches a minimum. As the chemical potential increases, the β'' minimum also shifts to the high-frequency region and becomes deeper. In the high-frequency region, absorption also increases

with increasing frequency, both due to the presence of unfilled energy levels in the graphene valence band and due to the radiative mode of plasmon-polariton propagation.

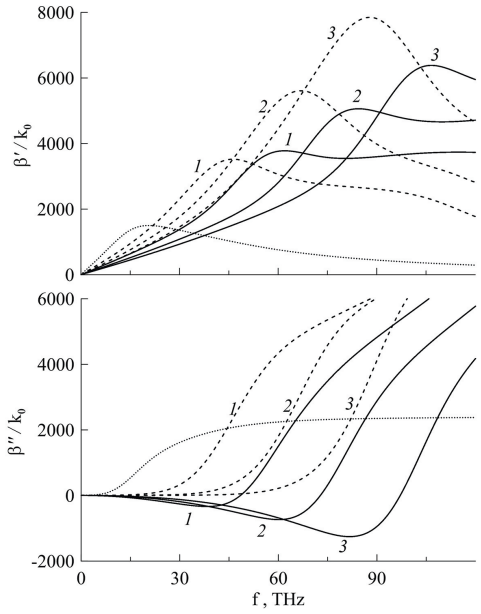

Fig. 2. Frequency dependence of the real and imaginary parts of the propagation constant of inverted and doped graphene (solid and dashed lines) in the case $\mu_1 = \mu_2 = 0,\ 0.10,\ 0.15,\ 0.20\, eV$ (dotted line, curves 1 – 3)

Fig. 3 shows the frequency dependences of the real and imaginary parts of the propagation constant of structures with inverted and doped graphene (solid and dotted lines) in the case of asymmetric excitation of graphene layers: $\mu_2 = 0,\ 0.10,\ 0.15,\ 0.20\ eV$, $\mu_1 = 0$ (dotted line, curves 1-3). A comparison of the symmetric and asymmetric regimes of inverted excitation of graphene layers shows that in the vicinity of the negative real part of the conductivity, with one-sided control, the plasmon-polariton propagation mode is realized with a higher amplification and a smaller phase shift than with two-sided control. In the case of asymmetric control, in addition to the existing mechanisms of recombination of charge carriers in inverted graphene, an additional potential difference arises between the plates, leading to charge tunneling from the valence band of the unexcited graphene layer to the valence band of inverted graphene through the dielectric barrier layer at a charge carrier energy sufficient for such a jump. There is also a jump between adjacent branches of solutions obtained numerically, which indirectly indicates the existence of more than one mode [31] in the considered frequency region at the current thickness of the barrier layer. In the complete absence of conductivity in equation (7), there are no solutions at all in this region.

In the case of layers of doped graphene with an asymmetric regime of control of the plates potentials in the same resonance region, a peak in the absorption of photons by graphene electrons is observed along with a phase incursion of a similar amplitude $\beta^{'}$. In the intrinsic absorption region of graphene, the discrepancies in the curves are more significant, since in the symmetric equilibrium case, the graphene valence band remains almost completely filled. The presence of a potential difference between the plates also provides the possibility of tunneling through the barrier layer to higher energy levels in the conduction band.

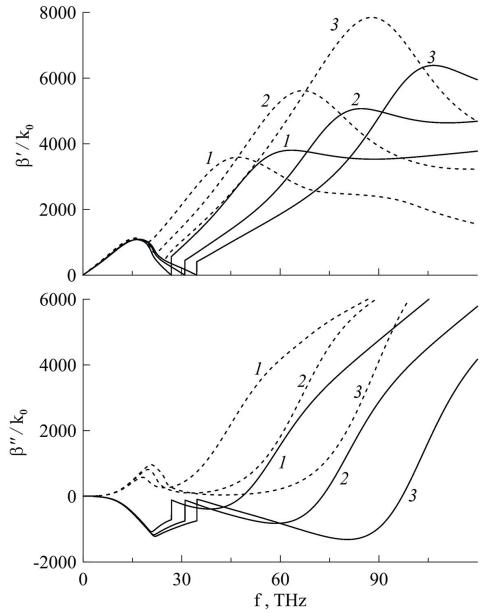

Fig. 3. Frequency dependence of the real and imaginary parts of the propagation constant of inverted and doped graphene (solid and dashed lines) in the case $\mu_1 = 0$, $\mu_2 = 0.10,\ 0.15,\ 0.20\ eV$ (curves 1 – 3)

Fig. 4 shows the frequency dependences of the group velocity in the case of the inverted (top) and doped (bottom) state of graphene sheets under different control modes, namely: $\mu_1 = \mu_2 = 0$ — dotted line, $\mu_1 = \mu_2 = \mu$ — solid lines, $\mu_1 = 0$, $\mu_2 = \mu$ — dashed line, $\mu = 0.10,\ 0.15,\ 0.20\ eV$ (curves 1 – 3). Propagating waves have an extremely low, including negative, group velocity in the considered frequency range. With an inverted population of levels in graphene, an increase in the potential causes a gradual expansion of the region of negative group velocity both for the same potentials on the graphene layers and for different ones. It is essential that in the presence of a potential difference between the plates, there is a section of positive group velocity in the amplification region, that is, a wave propagating in the forward direction and growing in amplitude takes place. For a doped state in this region, the group velocity loses its physical meaning, since the wave energy under equilibrium conditions is absorbed by free electrons in graphene. The shape of the curves for propagation constants and group velocities indicates the existence of a surface plasmon-polariton mode in the structure.

One of the important characteristics of surface waves is the depth of occurrence relative to the surface on which the wave is localized. Inside the waveguide, the sum of two modes localized on the corresponding graphene layers represents a single plasmon-polariton mode. The modes corresponding to equation (7a) will be called antisymmetric, and those corresponding to equation (7b) will be called symmetric, in accordance with the distribution relative to the symmetry plane of the longitudinal (tangential) field component E_x. Fig. 5 shows the distribution of three components of the TM wave field along the normal to the interface between the media, constructed using relations (2) and (7a) for various values of the barrier layer thickness ($d = 10,\ 14,\ 18,\ 22\ nm$) and $\mu = 0.10\ eV$, $f = 20\ THz$. It can be seen that at the layer boundaries (i.e., on graphene sheets), the wave magnetic field and the normal component of the electric field suffer a break due to the presence of boundary currents, and the components themselves are

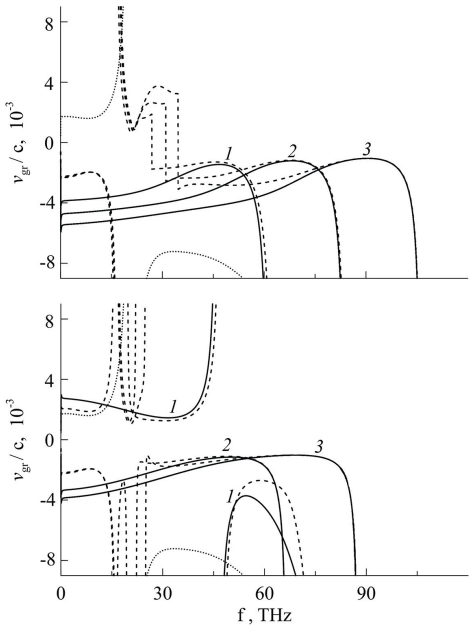

Fig. 4. Frequency dependences of the group velocity in the structure with inverted and doped graphene under different control regimes: $\mu_1 = \mu_2 = 0$ — dotted line, $\mu_1 = \mu_2 = \mu$ — solid lines, $\mu_1 = 0$, $\mu_2 = \mu$ — dashed lines, $\mu = 0.10,\ 0.15,\ 0.20\ eV$ (curves 1 – 3)

symmetric, while the tangential component of the electric field is continuous and antisymmetric. The surfaces of the waveguide are assumed to be electrically neutral. As the thickness of the barrier layer increases, the amplitudes of all components of the total wave field decrease, which is associated with a decrease in the overlap of fields localized on each of the graphene sheets.

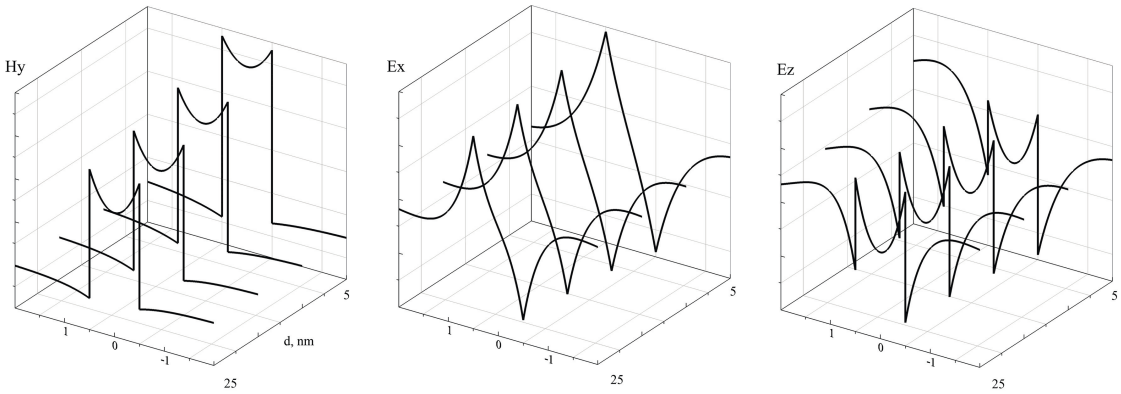

Fig. 5. Distribution of the TM wave field components over the waveguide thickness at $f = 20\ THz$, $\mu = 0.10\ eV$ and $d = 10,\ 14,\ 18,\ 22\ nm$

Fig. 6 shows the frequency dependence of the depth of the surface plasmon polariton outside the waveguide for inverted (top) and doped (bottom) graphene sheets under different control regimes: $\mu_1 = \mu_2 = 0$ — dotted line, $\mu_1 = \mu_2 = \mu$ — solid lines, $\mu_1 = 0$, $\mu_2 = \mu$ — dashed lines, $\mu = 0.10,\ 0.15,\ 0.20\ eV$ (curves 1 – 3). The case of unexcited graphene is characterized

by the existence of a strongly localized mode near the frequency of the minimum real part of the conductivity; when moving away from it, the plasmon-polariton loses its localization in all directions and turns into an radiative mode. The presence of excitation forces nonequilibrium charge carriers to screen the field of the mode propagating in the waveguide in a much wider frequency range both in the case of inverted graphene and in the case of doped graphene. The presence of a potential difference between the plates separates the frequency region of localization by the resonance peak. In the figure below, the discontinuity of the curves is caused by a jump from one sheet of the complex function to another in the numerical solution of the dispersion equations. In the case of doped graphene, this resonance has a finite height, which increases with the chemical potential. Obviously, with its growth, more and more electrons are distributed over high-energy levels, absorbing the energy of the plasmon-polariton, freeing up places at lower energy levels in the conduction band.

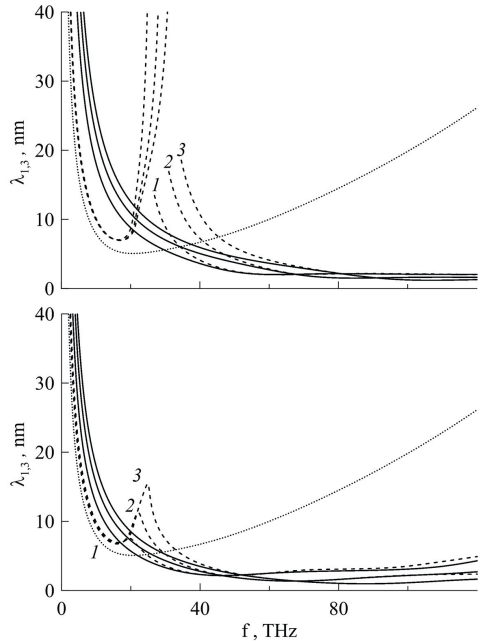

Fig. 6. Frequency dependence of the depth of the surface plasmon polariton outside the waveguide for inverted (top) and doped (bottom) graphene under different control regimes: $\mu_1 = \mu_2 = 0$ — dotted line, $\mu_1 = \mu_2 = \mu$ — solid lines, $\mu_1 = 0$, $\mu_2 = \mu$ — dashed lines, $\mu = 0.10,\ 0.15,\ 0.20\ eV$ (curves 1 – 3)

A more detailed analysis of the dispersion relations for the antisymmetric plasmon modes of the structure under consideration at various values of the parameters showed that additional modes arise in a limited frequency range, i.e. in a certain range of parameters, there is a modal bistability [31]. In this case, two modes are realized, which differ not only in the value of the propagation constant, but also in the sign of the group velocities (in narrower parameter intervals). The phase velocity of these modes decreases strongly in the cutoff region ($\beta^{'} \leqslant 0.1\ Mm^{-1}$). In the region of parameter values close to the mode cutoff, the group velocities of the modes entering the bistability have opposite signs, which can be used to create terahertz radiation generators based on two-layer graphene structures. The appearance of additional modes is characteristic of a two-layer graphene structure, and they were found both in the case of doped and inverted

graphene, as well as in the absence of excitation of graphene layers. In the case of inverted graphene, additional modes occur in the frequency range where mode amplification takes place. With a significant increase in the thickness of the barrier layer, the graphene layers can be considered isolated, and additional modes disappear. Additional modes are absent in structures with a single graphene layer. These modes are also absent for symmetric plasmons.

Conclusion

In this work, dispersion relations for plasmon-polariton surface modes in a symmetric planar structure consisting of two layers of doped or inverted graphene separated by a dielectric barrier layer are obtained in general form, and their numerical analysis is carried out. The possibility of controlling their dispersion properties by changing the chemical potential of graphene layers for different parameters of the barrier layer is shown. It is shown that the region of amplified waves existence in a structure with inverted graphene layers expands with an increase in the value of the chemical potential. In this case, the maximum value of the amplification factor not only increases, but also shifts up in frequency. An increase in the dielectric constant of the layer also contributes to amplification, since near the graphene layers on the side of the guide layer, the polarization of the dielectric has a significant effect.

It was also found that in a limited frequency range, in the presence of a potential difference between graphene layers, several modes exist at once, revealed due to a jump from one sheet of the complex function of the dispersion equation to another when it is solved numerically. The existence of detected additional modes does not critically depend on specific values of graphene conductivity, but disappears at a lower dielectric constant of the barrier layer. The effect has a clear generality for two-layer graphene structures, since it is observed in different energy states of graphene.

References

[1] K.S.Novoselov, A.K.Geim, S.V.Morozov, D.Jiang, M.I.Katsnelson, I.Grigorieva, S.Dubonos, A.Firsov, Two-dimensional gas of massless Dirac fermions in graphene, *Nature*, **438**(2005), 197–200. DOI: 10.1038/nature04233

[2] Y.Zhang, Y.W.Tan, H.L.Stormer, P.Kim, Experimental observation of the quantum Hall effect and Berry's phase in graphene, *Nature*, **438**(2005), 201–204. DOI: 10.1038/nature04235

[3] S.V.Morozov, K.S.Novoselov, A.K.Geim, Electron transport in graphene, *Physics–Uspekhi*, **51**(2008), 744–748. DOI: 10.3367/UFNr.0178.200807i.0776

[4] L.A.Falkovsky, Optical properties of graphene and IV-VI semiconductors, *Physics–Uspekhi*, **51**(2008), 887–897. DOI: 10.1070/PU2008v051n09ABEH006625

[5] V.Y.Aleshkin, A.A.Dubinov, V.Ryzhii, Terahertz laser based on optically pumped graphene: model and feasibility of realization, *Jetp Letters*, **89**(2009), 63–67. DOI: 10.1134/S0021364009020039

[6] A.C.Neto, F.Guinea, N.M.Peres, K.S.Novoselov, A.K.Geim, The electronic properties of graphene, *Reviews of modern physics*, **81(1)**(2009), 109–162.

[7] S.D.Sarma, S.Adam, E.Hwang, E.Rossi, Electronic transport in two-dimensional graphene, *Reviews of modern physics*, **83**(2011), 407–470.

[8] V.Popov, O.Polischuk, A.Davoyan, V.Ryzhii, T.Otsuji, M.Shur, Plasmonic terahertz lasing in an array of graphene nanocavities, *Physical review B*, **86**(2012), 195437. DOI: 10.1103/PhysRevB.86.195437

[9] I.V.Iorsh, I.Shadrivov, P.A.Belov, Y.S.Kivshar, Tunable hybrid surface waves supported by a graphene layer, *JETP letters*, **97**(2013), 249–252. DOI: 10.1134/S002136401305007X

[10] D.Smirnova, P.Buslaev, I.Iorsh, I.V.Shadrivov, P.A.Belov, Y.S.Kivshar, Deeply subwavelength electromagnetic Tamm states in graphene metamaterials, *Physical Review B*, **89**(2014), 245414. DOI: 10.1103/PhysRevB.89.245414

[11] A.Abramov, D.Evseev, D.Sementsov, Dispersion of a surface plasmon polaritons in a thin dielectric films surrounded by a two graphene layers, *Optik*, **195**(2019), 163105. DOI: 10.1016/j.ijleo.2019.163105

[12] G.Alymov, V.Vyurkov, V.Ryzhii, A.Satou, D.Svintsov, Auger recombination in Dirac materials: A tangle of many-body effects, *Physical Review B*, **97**(2018), 205411. DOI: 10.1103/PhysRevB.97.205411

[13] V.Ryzhii, M.Ryzhii, T.Otsuji, Negative dynamic conductivity of graphene with optical pumping, *Journal of Applied Physics*, **101**(2007), 083114. DOI: 10.1063/1.2717566

[14] A.Satou, F.Vasko, V.Ryzhii, Nonequilibrium carriers in intrinsic graphene under interband photoexcitation, *Physical Review B*, **78**(2008), 115431. DOI: 10.1103/PhysRevB.78.115431

[15] A.A.Dubinov, V.Y.Aleshkin, M.Ryzhii, T.Otsuji, V.Ryzhii, Terahertz laser with optically pumped graphene layers and Fabri–Perot resonator, *Applied physics express*, **2**(2009), 092301. DOI: 10.1143/APEX.2.092301

[16] A.Satou, V.Ryzhii, Y.Kurita, T.Otsuji, Threshold of terahertz population inversion and negative dynamic conductivity in graphene under pulse photoexcitation, *Journal of Applied Physics*, **113**(2013), 143108. DOI: 10.1063/1.4801916

[17] N.Yanushkina, M.Belonenko, N.Lebedev, Amplification of ultimately-short pulses in graphene in the presence of a high-frequency field, *Optics and spectroscopy*, **108**(2010), 618–623. DOI: 10.1134/S0030400X1004017X

[18] A.A.Dubinov, V.Y.Aleshkin, V.Mitin, T.Otsuji, V.Ryzhii, Terahertz surface plasmons in optically pumped graphene structures, *Journal of Physics: Condensed Matter*, **23**(2011), 145302. DOI: 10.1088/0953-8984/23/14/145302

[19] F.Rana, Graphene terahertz plasmon oscillators, *IEEE Transactions on Nanotechnology*, **7**(2008), 91–99. DOI: 10.1109/TNANO.2007.910334

[20] E.Hwang, S.D.Sarma, Screening-induced temperature-dependent transport in two-dimensional graphene, *Physical Review B*, **79**(2009), 165404.

[21] P.Buslaev, I.V.Iorsh, I.Shadrivov, P.A.Belov, Y.S.Kivshar, Plasmons in waveguide structures formed by two graphene layers, *JETP letters*, **97**(2013), 535–539. DOI: 10.1134/S0021364013090063

[22] C.H.Gan, H.S.Chu, E.P.Li, Synthesis of highly confined surface plasmon modes with doped graphene sheets in the midinfrared and terahertz frequencies, *Physical Review B*, **85**(2012), 125431. DOI: 10.1103/PhysRevB.85.125431

[23] M.Y.Morozov, I.Moiseenko, V.Popov, Giant amplification of terahertz plasmons in a double-layer graphene, *Journal of Physics: Condensed Matter*, **30**(2018), 08LT02. DOI: 10.1088/1361-648X/aaa648

[24] O.Polischuk, D.Fateev, V.Popov, On the Amplification of Terahertz Radiation by High-Q Resonant Plasmons in a Periodic Graphene Bilayer under Plasmon-Mode Anticrossing, *Semiconductors*, **53**(2019), 1211–1216. DOI: 10.1134/S106378261909015X

[25] E.Kukhar, S.Kryuchkov, Propagation of Plasmons in a Graphene Bilayer in a Transverse Electric Field, *Physics of the Solid State*, **62**(2020), 196–199.

[26] A.R.Davoyan, M.Y.Morozov, V.V.Popov, A.Satou, T.Otsuji, Graphene surface emitting terahertz laser: diffusion pumping concept, *Applied Physics Letters*, **103**(2013), 251102. DOI: 10.1063/1.4850522

[27] M.Y.Morozov, A.R.Davoyan, I.M.Moiseenko, A.Satou, T.Otsuji, V.V.Popov, Active guiding of Dirac plasmons in graphene, *Applied Physics Letters*, **106**(2015), 061105. DOI: 10.1063/1.4907644

[28] L.Falkovsky, A.Varlamov, Space-time dispersion of graphene conductivity, *The European Physical Journal B*, **56**(2007), 281–284. DOI: 10.1140/epjb/e2007-00142-3

[29] M.Y.Morozov, I.M.Moiseenko, A.V.Korotchenkov, V.Popov, Deceleration of terahertz plasma waves in tapered structure with graphene pumped by using optical plasmons, *Fizika i Tekhnika Poluprovodnikov*, **55**(2021), 518–523 (in Russian). DOI: 10.21883/FTP.2021.06.50920.9525

[30] O.Polischuk, D.Fateev, V.Popov, Electrical tunability of terahertz amplification in a periodic plasmon graphene structure with charge-carrier injection, *Semiconductors*, **52**(2018), 1534–1539. DOI: 10.1134/S1063782618120187

[31] A.M.Shutyi, D.I.Sementsov, S.V.Eliseeva, Mode bistability of plasmons and a dispersive jump in a structure with two graphene layers, *Physics of the Solid State*, **64(6)**(2022), 724–731 (in Russian). DOI: 10.21883/FTT.2022.06.52407.259

Поверхностные плазмон-поляритоны в двуслойной графеновой структуре с диэлектрическим барьерным слоем при различных режимах управления

Дмитрий А. Евсеев
Светлана В. Елисеева
Анатолий М. Шутый
Дмитрий И. Семенцов
Ульяновский государственный университет
Ульяновск, Российская Федерация

Аннотация. Сравниваются дисперсионные зависимости симметричного диэлектрического волновода с графеновыми обкладками в двух режимах управления потенциалом графена с двух сторон структуры. Получено общее дисперсионное соотношение, численный анализ которого выявил возможность управления параметрами усиливаемых поверхностных мод. Проведен численный анализ решений дисперсионного соотношения в случае симметрии и асимметрии управляющего потенциала на графеновых слоях. В области отрицательной проводимости графена при наличии инверсной населенности уровней обнаружено решение, растущее по амплитуде во времени.

Ключевые слова: допированный и инвертированный графен, терагерцовый диапазон частот, симметричная планарная структура, химпотенциал, действительная и мнимая части константы распространения, усиление.